Uniform electron gases. II. The generalized local density approximation in one dimension

Pierre-François Loos, Caleb J. Ball, and Peter M. W. Gill
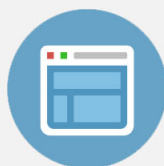
Uniform electron gases. II. The generalized local density approximation in one dimension

Pierre-François Loos,[a] Caleb J. Ball, and Peter M. W. Gill[b]
Research School of Chemistry, Australian National University, Canberra ACT 0200, Australia

We introduce a generalization (gLDA) of the traditional Local Density Approximation (LDA) within density functional theory. The gLDA uses both the one-electron Seitz radius r_s and a two-electron hole curvature parameter η at each point in space. The gLDA reduces to the LDA when applied to the infinite homogeneous electron gas but, unlike the LDA, it is also exact for finite uniform electron gases on spheres. We present an explicit gLDA functional for the correlation energy of electrons that are confined to a one-dimensional space and compare its accuracy with LDA, second- and third-order Møller-Plesset perturbation energies, and exact calculations for a variety of inhomogeneous systems. © 2014 AIP Publishing LLC. [http://dx.doi.org/10.1063/1.4867910]

I. LOCAL DENSITY APPROXIMATION

The local density approximation (LDA), unlike most of the "sophisticated" density functional approximations in widespread use today, is truly a first-principles quantum mechanical method.[1] It is entirely non-empirical, depending instead on the properties of one of the great paradigms of modern physics: the infinite homogeneous electron gas (HEG).[2,3] Application of the LDA is straightforward, at least in principle. Although the electronic charge density $\rho(\mathbf{r})$ in any real system is non-uniform, the LDA proceeds by assuming that the charge in an infinitesimal volume element around the point $\mathbf{r}$ behaves like a locally homogeneous gas of density $\rho(\mathbf{r})$, and adds all of the resulting contributions together. This implicitly assumes that the infinitesimal contributions are independent (which is undoubtedly not the case) but then requires only that the properties of the HEG be known for all values of ρ.

The density of a HEG is commonly given by ρ (the number of electrons per unit volume) or the Seitz radius r_s and these equivalent parameters are related by

$$r_s^{\mathcal{D}} \rho = \pi^{-\mathcal{D}/2} \Gamma(\mathcal{D}/2 + 1), \tag{1}$$

where $\mathcal{D}$ is the dimensionality of the space in which the electrons move. In terms of these, the LDA correlation functional is

$$E_c^{\text{LDA}} = \int \rho(\mathbf{r}) \varepsilon_c(r_s(\mathbf{r})) \, d\mathbf{r}, \tag{2}$$

where the correlation kernel $\varepsilon_c(r_s)$ is the reduced (i.e., per electron) correlation energy of the HEG with Seitz radius r_s.

In high-density HEGs (i.e., $r_s \ll 1$), the kinetic energy dominates the Hamiltonian and the Coulomb repulsion between the electrons can be treated via perturbation theory. This has facilitated investigations of $\varepsilon_c(r_s)$ in 3D[4–19] and 2D[20–29] but, because the Coulomb operator is so strong in 1D

that two electrons cannot touch, the 1D gas has received less attention.[30–32]

In low-density HEGs (i.e., $r_s \gg 1$), the potential energy dominates, the electrons localize into a Wigner crystal and strong-coupling methods can be used to find asymptotic expansions of $\varepsilon_c(r_s)$. Here, too, the 3D,[33–35] 2D,[36,37] and 1D[30] HEGs have all been studied.

For intermediate densities, the best estimates of $\varepsilon_c(r_s)$ come from Quantum Monte Carlo (QMC) calculations, as pioneered by Ceperley and refined by several other groups.[38–53] By combining these with the high- and low-density results, various groups[54–57] have constructed interpolating functions that allow $\varepsilon_c(r_s)$ to be estimated rapidly for any value of r_s.

Unfortunately, this approach is flawed, for the correlation energy of a uniform electron gas depends on more than just its r_s value.[58] We have therefore argued that $\varepsilon_c(r_s)$ should be generalized to $\varepsilon_c(r_s, \eta)$, where the parameter η measures the *two-electron* density. Although not mathematically mandated,[59] we prefer that η, like r_s, be a *local* quantity. In Sec. II, we propose a definition for η inspired by a number of previous researchers.[60–64]

To learn more about the two-parameter kernel, we have turned to the finite uniform electron gases (UEGs) formed when n electrons are confined to a $\mathcal{D}$-sphere.[65–72] In Sec. III, we report accurate values of η and $\varepsilon_c(r_s, \eta)$ for electrons on a 1-sphere, systems that we call "n-ringium." In Sec. IV, we devise three functionals to approximate these results and in Sec. V, we test two of these on small 1D systems. Atomic units are used throughout.

II. HOLE CURVATURE

Suppose that an electron lies at a point $\mathbf{r}$. The probability $P(\mathbf{u}|\mathbf{r})$ that a second electron lies at $\mathbf{r} + \mathbf{u}$ is given[60,61,73–82] by the conditional intracule

$$P(\mathbf{u}|\mathbf{r}) = \rho_2(\mathbf{r}, \mathbf{r} + \mathbf{u})/\rho(\mathbf{r}) = [\rho(\mathbf{r} + \mathbf{u}) + \rho_{\text{xc}}(\mathbf{r}, \mathbf{r} + \mathbf{u})]/2, \tag{3}$$

where ρ_{xc} is the exchange-correlation hole[1] and

[a] Electronic mail: pf.loos@anu.edu.au
[b] Electronic mail: peter.gill@anu.edu.au

$$\rho_2(\mathbf{r}_1, \mathbf{r}_2) = n(n-1) \int |\Psi|^2 \, ds_1 ds_2 d\mathbf{r}_3 \ldots d\mathbf{r}_n \quad (4)$$

is the spinless second-order density matrix.[83] For fixed $\mathbf{r}$, we have the normalization

$$\int P(\mathbf{u}|\mathbf{r}) \, d\mathbf{u} = n - 1. \quad (5)$$

Because the Laplacian $\nabla_\mathbf{u}^2 P(\mathbf{0}|\mathbf{r})$ measures the tightness of the hole around the electron at $\mathbf{r}$ and has dimensions of $1/(\text{length})^{\mathcal{D}+2}$, we can use the dimensionless hole curvature

$$\eta(\mathbf{r}) = C_\mathcal{D} \, r_s(\mathbf{r})^{\mathcal{D}+2} \, \nabla_\mathbf{u}^2 P(\mathbf{0}|\mathbf{r}) \quad (6)$$

to measure the proximity of other electrons to one at $\mathbf{r}$. (We will fix the coefficient $C_\mathcal{D}$ in Sec. III A.) It is difficult to find this Laplacian for the exact wave function but, at the Hartree-Fock (HF) level, it involves simple sums over the occupied orbitals, viz.

$$\nabla_\mathbf{u}^2 P(\mathbf{0}|\mathbf{r}) = 2 \sum_i^{\text{occ}} |\nabla \psi_i|^2 - \frac{|\nabla \rho|^2}{2\rho} \quad (7)$$

and we will therefore employ HF curvatures henceforth.[84] The interesting connection between the curvature and the kinetic energy density[62] is worth noting.

III. CALCULATIONS ON n-RINGIUM

A. Density and curvature

The HF orbitals of the ground state of n electrons on a ring of radius R are complex exponentials[71,72]

$$\psi_m(\theta) = (2\pi R)^{-1/2} \exp(im\theta), \quad (8)$$

$$m = -\frac{n-1}{2}, -\frac{n-3}{2}, \ldots, +\frac{n-3}{2}, +\frac{n-1}{2}, \quad (9)$$

and, because of the symmetry of the system, the density and Seitz radius

$$\rho = n/(2\pi R), \quad (10)$$

$$r_s = \pi R/n \quad (11)$$

do not depend on θ. The hole curvature is also constant and, using (6) and (7), one finds

$$\eta = 2C_1(\pi R/n)^3 \sum_m^{\text{occ}} m^2/(2\pi R^3)$$

$$= C_1(\pi^2/12)(1 - 1/n^2). \quad (12)$$

If we choose $C_1 = 12/\pi^2$ so that $\eta = 1$ for the 1D HEG (i.e., ∞-ringium), we obtain

$$\eta = 1 - 1/n^2. \quad (13)$$

In general, requiring that $\eta = 1$ in the $\mathcal{D}$-dimensional HEG leads (via Fermi integration) to

$$C_\mathcal{D} = \frac{(1 + 2/\mathcal{D})\pi^{\mathcal{D}/2}/8}{\Gamma(1 + \mathcal{D}/2)^{1+4/\mathcal{D}}} \quad (14)$$

and the particular values $C_2 = \pi/4$ and $C_3 = (10/27)(4\pi/3)^{1/3}$.

B. Correlation energy

The Hamiltonian for n electrons on a ring is

$$\hat{H} = \hat{T} + \hat{V} = -\frac{1}{2} \sum_{i=1}^n \nabla_i^2 + \sum_{i<j}^n r_{ij}^{-1}, \quad (15)$$

where r_{ij} is the distance (across the ring) between electrons i and j. As noted previously,[72] the energy is independent of the spin-state and so we assume that all electrons are spin-up. The exact wave function can then be written as $\Psi = F\Phi$, where the correlation factor

$$F = \sum_{a=1}^\infty x_a f_a \quad (16)$$

is a sum of functions f_a which are m_a-term symmetric polynomials in the r_{ij} (see Table I) and Φ is the HF wave function[72]

$$\Phi = \frac{1}{\sqrt{n!(2\pi)^n}} \prod_{i<j}^n \hat{r}_{ij}. \quad (17)$$

Judicious integration by parts allows us to partition the total energy

$$E = \frac{\langle \Psi | \hat{H} | \Psi \rangle}{\langle \Psi | \Psi \rangle} \quad (18)$$

into the HF energy[72]

$$E_{\text{HF}} = T_{\text{HF}} + V_{\text{HF}}$$

$$= \frac{n(n^2-1)}{24R^2} + \frac{1}{4\pi R} \left(\sum_{k=1}^n \frac{4n^2-1}{2k-1} - 3n^2 \right) \quad (19)$$

TABLE I. Definitions f_a and number of terms m_a in the correlation factors of degree 0, 1, 2, 3.

Degree 0		Degree 1		Degree 2		Degree 3	
f_1	m_1	f_2	m_2	$f_3 \ldots f_5$	$m_3 \ldots m_5$	$f_6 \ldots f_{13}$	$m_6 \ldots m_{13}$
1	1	$\sum r_{ij}$	$_n\mathrm{C}_2$	$\sum r_{ij}^2$	$_n\mathrm{C}_2$	$\sum r_{ij}^3$	$_n\mathrm{C}_2$
				$\sum r_{ij} r_{ik}$	$6\,_n\mathrm{C}_3$	$\sum r_{ij} r_{ik} r_{jk}$	$6\,_n\mathrm{C}_3$
				$\sum r_{ij} r_{kl}$	$6\,_n\mathrm{C}_4$	$\sum r_{ij}^2 r_{ik}$	$18\,_n\mathrm{C}_3$
						$\sum r_{ij}^2 r_{kl}$	$18\,_n\mathrm{C}_4$
						$\sum r_{ij} r_{ik} r_{il}$	$24\,_n\mathrm{C}_4$
						$\sum r_{ij} r_{ik} r_{jl}$	$72\,_n\mathrm{C}_4$
						$\sum r_{ij} r_{ik} r_{lm}$	$180\,_n\mathrm{C}_5$
						$\sum r_{ij} r_{kl} r_{mn}$	$90\,_n\mathrm{C}_6$
Total 1	1	$\sum r_{ij}$	$_n\mathrm{C}_2$	$(\sum r_{ij})^2$	$(_n\mathrm{C}_2)^2$	$(\sum r_{ij})^3$	$(_n\mathrm{C}_2)^3$

TABLE II. η and $-\varepsilon_c(r_s, \eta)$ (mE_h per electron) for the ground state of n electrons on a ring.

n	η	\(r_s\) 0	1/10	1/5	1/2	1	2	5	10	20	50	100
1	0	0	0	0	0	0	0	0	0	0	0	0
2	3/4	13.212	12.985	12.766	12.152	11.250	9.802	7.111	4.938	3.122	1.533	0.848
3	8/9	18.484	18.107	17.747	16.755	15.346	13.179	9.369	6.427	4.030	1.965	1.083
4	15/16	21.174	20.700	20.250	19.027	17.324	14.765	10.391	7.087	4.425	2.150	1.184
5	24/25	22.756	22.216	21.706	20.332	18.444	15.648	10.947	7.441	4.636	2.249	1.237
6	35/36	23.775	23.190	22.638	21.161	19.148	16.196	11.285	7.655	4.774	2.307	1.268
7	48/49	24.476	23.855	23.273	21.723	19.618	16.557	11.509	7.795	4.844	2.345	1.289
8	63/64	24.981	24.328	23.729	22.122	19.951	16.813	11.664	7.890	4.901	2.370	1.302
9	80/81	25.360	24.686	24.067	22.415	20.199	17.001	11.777	7.960	4.941	2.389	1.312
10	99/100	25.651	24.960	24.327	22.644	20.386	17.143	11.857	8.013	4.973	2.404	1.320
∞	1	27.416	26.597	25.91	23.962	21.444	17.922	12.318	8.292	5.133	2.476	1.358

and the correlation energy

$$E_c = \frac{\langle \Phi \mid \frac{1}{2}\nabla F \cdot \nabla F + (\hat{V} - V_{HF})F^2 \mid \Phi \rangle}{\langle \Phi | F^2 | \Phi \rangle}. \quad (20)$$

E_c can be minimized either by QMC methods[52] or via the secular equation

$$(\mathbf{T} + \mathbf{V})\mathbf{x} = E_c \, \mathbf{S} \, \mathbf{x}, \quad (21)$$

where the overlap, kinetic, and Coulomb matrix elements

$$S_{ab} = \langle \Phi | f_a f_b | \Phi \rangle, \quad (22a)$$

$$T_{ab} = \frac{1}{2}\langle \Phi | \nabla f_a \cdot \nabla f_b | \Phi \rangle, \quad (22b)$$

$$V_{ab} = \langle \Phi | f_a \hat{V} f_b | \Phi \rangle - V_{HF} S_{ab} \quad (22c)$$

can be found analytically in Fourier space (Appendix A). We have used the CASINO QMC package[85] and, where possible, the Knowles–Handy full CI program to confirm results.[86,87]

Table II shows the resulting near-exact correlation energies for ground-state n-ringium. (Where these energies differ from those in Table VI of Ref. 72, the new values are superior.) The fact that the ε_c values in a given column are not equal demonstrates that the correlation energy of a UEG is not determined by its r_s value alone.[58] Moreover, the variations in ε_c for a given r_s are large: the $n = 2$ values, for example, are only about half of the $n = \infty$ values, implying that the correlation energy of a few-electron system is grossly overestimated by the LDA functional which is based on the HEG.

IV. GENERALIZED LOCAL DENSITY APPROXIMATION

In the LDA, the correlation contribution is estimated from r_s alone, according to Eq. (2). However, the fact that UEGs with the same r_s, but different η, have different energies compels us to devise a Generalized Local Density Approximation (GLDA) wherein we write

$$E_c^{GLDA} = \int \rho(\mathbf{r}) \, \varepsilon_c(r_s(\mathbf{r}), \eta(\mathbf{r})) \, d\mathbf{r}, \quad (23)$$

where the correlation kernel $\varepsilon_c(r_s, \eta)$ is the reduced correlation energy of a UEG with Seitz radius r_s and curvature η.

For present purposes, we will use r_s and η values from the HF, rather than the exact, wave function.

One might think that the kernel could be constructed by fitting the results in Table II but these data allow us to construct $\varepsilon_c(r_s, \eta)$ only for $\eta \leq 1$. To construct the rest of the kernel will require accurate correlation energies for uniform gases with high curvatures ($\eta > 1$) but, although these arise in *excited* states of n-ringium, this raises some fundamental questions which lie outside the scope of the present manuscript and will be discussed elsewhere.

A. High densities

Rayleigh-Schrödinger perturbation theory for n-ringium yields the high-density expansion

$$\varepsilon_c(r_s, n) = \alpha_2(n) + \alpha_3(n)r_s + \alpha_4(n)r_s^2 + \ldots, \quad (r_s \ll 1). \quad (24)$$

The leading coefficient[72] is

$$\alpha_2(n) = -\frac{1}{n} \sum_{a<b}^{occ} \sum_{r=r_{min}}^{\infty} \frac{V_{r-a,r-b}^2}{(r-a)(r-b)}$$

$$= -\frac{\pi^2}{360} + \frac{a \ln^2 n + b \ln n + c}{n^2} + \ldots \quad (25)$$

but, if we fit a truncated version of this series, while ensuring that α_2 vanishes for one electron, we obtain the approximation

$$\tilde{\alpha}_2(n) = -\frac{\pi^2}{360}\left(1 - \frac{1}{n^2}\right) + \frac{\ln^2 n + 3 \ln n}{87n^2} \quad (1 \leq n < \infty), \quad (26)$$

which can be rewritten in terms of the curvature, using Eq. (13) to obtain

$$\tilde{\alpha}_2(\eta) = -\frac{\pi^2}{360}\eta + (1-\eta)\frac{\ln^2(1-\eta) - 6\ln(1-\eta)}{348}$$
$$(0 \leq \eta \leq 1). \quad (27)$$

The accuracy of this approximation is shown in columns 2 and 3 of Table III.

TABLE III. Application of the $\tilde{\varepsilon}_c(r_s, \eta)$ approximation to the data in Table II.

n	η	$-\alpha_2$	$-\tilde{\alpha}_2$	$-\beta_2$	$-\tilde{\beta}_2$	$\tilde{\gamma}$	Max errors %	Max errors Abs (mE$_h$)
2	3/4	0.01321	0.01321	0.1073	0.1050	1.9792	1.0	0.10
3	8/9	0.01848	0.01862	0.1361	0.1349	2.1375	0.9	0.13
4	15/16	0.02117	0.02133	0.1483	0.1475	2.2054	0.8	0.16
5	24/25	0.02276	0.02291	0.1546	0.1541	2.2431	0.8	0.18
6	35/36	0.02378	0.02391	0.1584	0.1580	2.2670	0.7	0.14
7	48/49	0.02448	0.02460	0.1608	0.1605	2.2837	0.8	0.16
8	63/64	0.02498	0.02509	0.1624	0.1622	2.2958	0.7	0.16
9	80/81	0.02536	0.02546	0.1636	0.1635	2.3051	0.7	0.15
10	99/100	0.02565	0.02574	0.1645	0.1644	2.3125	0.8	0.20
∞	1	0.02742	0.02742	0.1689	0.1689	2.3750	0.8	0.13

B. Low densities

Strong-coupling perturbation theory for n-ringium yields the low-density expansion

$$\varepsilon_c(r_s, n) = \frac{\beta_2(n)}{r_s} + \frac{\beta_3(n)}{r_s^{3/2}} + \frac{\beta_4(n)}{r_s^2} + \dots \quad (r_s \gg 1). \quad (28)$$

The leading coefficient is the difference between the Wigner crystal Coulomb coefficient

$$
\begin{aligned}
E_V^W(n) &= \frac{\pi}{4n} \sum_{k=1}^{n-1} \csc(k\pi/n) \\
&= \frac{1}{2} \int_0^1 \frac{1 - x^{n-1}}{1 - x} \frac{dx}{1 + x^n} \\
&= \frac{\ln n}{2} + \frac{\gamma + \ln(2/\pi)}{2} - \frac{\pi^2}{144n^2} + \dots \quad (29)
\end{aligned}
$$

and the HF Coulomb coefficient

$$
\begin{aligned}
E_V^{HF}(n) &= \left(1 - \frac{1}{4n^2}\right) \sum_{k=1}^{n} \frac{1}{2k-1} - \frac{3}{4} \\
&= \left(1 - \frac{1}{4n^2}\right)\left(\frac{\ln n}{2} + \frac{\gamma + 2\ln 2}{2} + \frac{1}{48n^2} + \dots\right) - \frac{3}{4}. \quad (30)
\end{aligned}
$$

It follows that

$$\beta_2(n) = \frac{3}{4} - \frac{\ln 2\pi}{2} + \frac{\ln n}{8n^2} + \frac{18\gamma + 36\ln 2 - 3 - \pi^2}{144n^2} + \dots \quad (31)$$

but, if we truncate this series after the n^{-2} term and modify it to ensure that β_2 vanishes for one electron, we obtain the approximation

$$\tilde{\beta}_2(n) = \left(\frac{3}{4} - \frac{\ln 2\pi}{2}\right)\left(1 - \frac{1}{n^2}\right) + \frac{\ln n}{8n^2} \quad (1 \le n < \infty), \quad (32)$$

which can be rewritten in terms of the curvature, using Eq. (13) to obtain

$$\tilde{\beta}_2(\eta) = \left(\frac{3}{4} - \frac{\ln 2\pi}{2}\right)\eta - \frac{(1 - \eta)\ln(1 - \eta)}{16} \quad (0 \le \eta \le 1). \quad (33)$$

The accuracy of this approximation is shown in columns 4 and 5 of Table III.

C. Intermediate densities

How can we model $\varepsilon_c(r_s, \eta)$ for fixed η? Ideally, we would like a function that reproduces the behaviors of Eqs. (24) and (28) and interpolates accurately between these limits. However, for practical reasons, we will content ourselves with a function that approaches $\tilde{\alpha}_2(\eta)$ for small r_s, behaves like $\tilde{\beta}_2(\eta)/r_s$ for large r_s, and changes monotonically between these.

Although we could use robust interpolation,[88] the hypergeometric function[89]

$$f(r) = \alpha F\left(1, \frac{3}{2}, \gamma, \frac{2\alpha(1 - \gamma)}{\beta}r\right) \quad (34)$$

$$\sim \begin{cases} \alpha + O(r) & r \ll 1 \\ \beta/r + O(r^{-3/2}) & r \gg 1 \end{cases} \quad (35)$$

possesses all of the desired features and we therefore adopt the approximate kernel

$$\tilde{\varepsilon}_c(r_s, \eta) = \tilde{\alpha}_2(\eta) F\left(1, \frac{3}{2}, \tilde{\gamma}(\eta), \frac{2\tilde{\alpha}_2(\eta)(1 - \tilde{\gamma}(\eta))}{\tilde{\beta}_2(\eta)}r_s\right). \quad (36)$$

Table III shows that this kernel models the energies in Table II well if we choose

$$\tilde{\gamma}(n) = \frac{19}{16}\left(\frac{4n-3}{2n-1}\right) \quad (1 \le n < \infty) \quad (37)$$

or, equivalently,

$$\tilde{\gamma}(\eta) = \frac{19}{16}\left(\frac{4 - 3\sqrt{1 - \eta}}{2 - \sqrt{1 - \eta}}\right) \quad (0 \le \eta \le 1). \quad (38)$$

This reproduces the Table II data to within a relative error of 1% and absolute error of 0.20 mE$_h$.

D. The LDA1, GLDA1, and gLDA1 functionals

We can now consider three approximate kernels for correlation in 1D systems. The first is the LDA1 kernel, which is

defined by

$$\varepsilon_c^{\text{LDA1}}(r_s) = \alpha F\left(1, \frac{3}{2}, \tilde{\gamma}, \frac{2\alpha(1-\tilde{\gamma})}{\beta} r_s\right), \qquad (39)$$

where $\alpha = -\pi^2/360$, $\beta = 3/4 - (\ln 2\pi)/2$, and $\tilde{\gamma} = 19/8$. This underpins the traditional LDA and, by construction, it is exact (within fitting errors) for the 1D HEG or, equivalently, for ∞-ringium. It is independent of the hole curvature η.

The second is the GLDA1 kernel, which is defined by

$$\varepsilon_c^{\text{GLDA1}}(r_s, \eta) = \tilde{\alpha}_2(\eta) F\left(1, \frac{3}{2}, \tilde{\gamma}(\eta), \frac{2\tilde{\alpha}_2(\eta)(1-\tilde{\gamma}(\eta))}{\tilde{\beta}_2(\eta)} r_s\right), \qquad (40)$$

where $\tilde{\alpha}_2(\eta)$, $\tilde{\beta}_2(\eta)$, and $\tilde{\gamma}(\eta)$ are defined in Eqs. (27), (33), and (38). Unfortunately, because of a lack of information about high-curvature UEGs, these three equations are not defined for $\eta > 1$ and thus, at this time, the GLDA1 is defined only for systems where $\eta \leq 1$ at all points. Completing the definition of the GLDA1 is an important topic for future work.

The third is the gLDA1 kernel, a partially corrected LDA, which is defined by

$$\varepsilon_c^{\text{gLDA1}}(r_s, \eta) = \begin{cases} \varepsilon_c^{\text{GLDA1}}(r_s, \eta) & \eta < 1 \\ \varepsilon_c^{\text{LDA1}}(r_s) & \eta \geq 1 \end{cases}. \qquad (41)$$

When applied to UEGs with $\eta \geq 1$, the gLDA1 and LDA1 kernels are, of course, identical. However, when applied to gases with $\eta < 1$, they behave differently and, by construction, the gLDA1 kernel is exact (within fitting errors) for any n-ringium.

The gLDA1 kernel defaults back to the LDA1 kernel at points where $\eta > 1$ but we cannot predict *a priori* whether this will cause it to underestimate or to overestimate the GLDA. If the monotonic increase in the magnitude of the kernel between $\eta = 0$ and $\eta = 1$ continues beyond $\eta = 1$, then the gLDA1 kernel (which assumes that the kernel is constant beyond $\eta = 1$) will underestimate the GLDA1 kernel and consequently underestimate the magnitude of the correlation energies in systems with high-curvature regions.

Until the true kernel for $\eta > 1$ is known, we cannot draw any firm conclusions about the accuracy of GLDA1. However, it is reasonable to conjecture that even the imperfect gLDA1 may be superior to LDA1 for density functional theory (DFT) calculations on inhomogeneous 1D systems and we now explore this through some preliminary validation studies.

V. VALIDATION

Having defined the gLDA1 functional, we turn now to its validation. The functional is exact by construction for any n-ringium, so we require systems with non-uniform densities. There is no standard set of 1D models with accurately known correlation energies, so it was necessary to devise our own and we chose the ground states of n electrons in a 1D box of length $L = \pi$ (a family that we call the n-boxiums) and of n electrons in a 1D harmonic well with force constant $k = 1$ (a family that we call the n-hookiums). Whereas the HOMO–LUMO gap in n-boxium increases roughly linearly with n,

TABLE IV. Basis set truncation errors ΔE_M for the energies in two-electron systems.

	MP2	MP3	FCI
2-ringium	$O(M^{-3})$	$O(M^{-3})$	$O(M^{-3})$
2-boxium	$O(M^{-3})$	$O(M^{-3})$	$O(M^{-3})$
2-hookium	$O(M^{-3/2})$	$O(M^{-3/2}/\ln M)$	$O(M^{-3/2})$

that in n-hookium slowly decreases. We therefore regard them as "large-gap" and "small-gap" systems, respectively.

Given that the fitting errors (Table III) in the gLDA1 functional can be of the order of 0.1 mE_h, we aimed to obtain the energies of the n-boxium and n-hookium to within 0.1 mE_h of their complete basis set (CBS) limits. This is easily achieved for the HF, LDA1, and gLDA1 energies, because they converge exponentially[90–92] with the size M of the one-electron basis, but it is less straightforward for traditional post-HF energies.

We analysed the convergence behavior (see Appendix B) of Møller-Plesset perturbation (MP2 and MP3) and full configuration interaction (FCI) energies in 2-ringium, 2-boxium, and 2-hookium and our results are summarised in Table IV. From these, we devised appropriate extrapolation formulae and applied these to the energies obtained with our largest basis sets. We also used QMC calculations[85] to assess the accuracy of our extrapolated FCI energies.

Tables V and VI show the energies obtained for 5-boxium and 5-hookium, respectively, as the basis set size increases from $M = 5$ to $M = 30$. The three components of the third-order energy are separated because of their different convergence behaviors. Table VII summarizes our best estimates of the HOMO–LUMO gaps, together with the HF, LDA1, gLDA1, MP2, MP3, and FCI energies, for n-boxium and n-hookium with $n = 2, 3, 4,$ or 5.

A. *n*-boxium

The 2-boxium system (albeit with length $L = 3$) was studied in a basis of delta functions by Salter *et al.*[93] and, using 804 609 basis functions, they obtained energies within roughly 10 μE_h of the exact values. The present work is the first study of n-boxium with $n \geq 3$.

The orbitals of 1-boxium are

$$\phi_m(x) = \begin{cases} \sqrt{2/\pi}\cos mx & m \text{ is odd} \\ \sqrt{2/\pi}\sin mx & m \text{ is even} \end{cases} \quad (m = 1, 2, 3, \ldots) \qquad (42)$$

and the first M of these form a convenient orthonormal basis for expanding the HF orbitals in n-boxium. The anti-symmetrized two-electron integrals $\langle \mu\sigma||\nu\lambda\rangle$ can be found in terms of the Sine and Cosine Integral functions[89] and we have used these to perform SCF calculations with up to $M = 30$ basis functions. Our convergence criterion was $\max |[\mathbf{P}, \mathbf{F}]| < 10^{-5}$.

TABLE V. Basis set convergence of E_{HF} (in E_h) and E_c energies (in mE_h) in 5-boxium.

M	E_{HF}	$-E_c^{LDA1}$	$-E_c^{gLDA1}$	$-E_c^{MP2}$	$E^{(3)}$ components			$-E_c^{FCI}$
					O^4V^2	O^3V^3	O^2V^4	
5	40.990 531	126.517	68.858	0	0	0	0	0
6	40.855 806	126.499	63.929	0	0	0	0	0
7	40.807 556	126.486	63.678	16.020	1.129	−3.512	0.804	17.840
8	40.798 066	126.482	63.314	28.753	1.728	−6.379	1.683	32.157
9	40.793 901	126.478	63.208	38.619	2.085	−8.570	2.475	43.234
10	40.793 518	126.478	63.207	45.564	2.276	−10.046	3.104	50.937
11	40.792 520	126.477	63.067	49.972	2.371	−10.871	3.577	55.640
12	40.792 237	126.477	63.024	53.055	2.426	−11.394	3.932	58.850
13	40.792 064	126.477	63.026	55.272	2.458	−11.729	4.203	61.102
14	40.792 057	126.477	63.031	56.876	2.478	−11.939	4.411	62.682
15	40.792 051	126.477	63.019	58.059	2.491	−12.071	4.572	63.815
16	40.792 051	126.477	63.017	58.946	2.499	−12.157	4.699	64.646
17	40.792 049	126.477	63.026	59.624	2.505	−12.214	4.799	65.271
18	40.792 049	126.477	63.027	60.151	2.509	−12.254	4.880	65.750
19	40.792 049	126.477	63.028	60.568	2.512	−12.282	4.945	66.124
20	40.792 048	126.477	63.028	60.901	2.514	−12.302	4.998	66.420
21	40.792 048	126.477	63.029	61.170	2.515	−12.317	5.042	66.658
22	40.792 048	126.477	63.029	61.391	2.516	−12.328	5.079	66.852
23	40.792 048	126.477	63.029	61.574	2.517	−12.337	5.110	67.011
24	40.792 048	126.477	63.029	61.726	2.517	−12.343	5.136	67.143
25	40.792 048	126.477	63.029	61.854	2.518	−12.349	5.158	67.253
26	40.792 048	126.477	63.029	61.963	2.518	−12.353	5.176	67.346
27	40.792 048	126.477	63.029	62.055	2.519	−12.356	5.193	67.425
28	40.792 048	126.477	63.029	62.134	2.519	−12.358	5.207	67.493
29	40.792 048	126.477	63.029	62.203	2.519	−12.360	5.219	67.551
30	40.792 048	126.477	63.029	62.262	2.519	−12.362	5.230	67.601

TABLE VI. Basis set convergence of E_{HF} (in E_h) and E_c energies (in mE_h) in 5-hookium.

M	E_{HF}	$-E_c^{LDA1}$	$-E_c^{gLDA1}$	$-E_c^{MP2}$	$E^{(3)}$ components			$-E_c^{FCI}$
					O^4V^2	O^3V^3	O^2V^4	
5	19.649 014	116.419	75.381	0	0	0	0	0
6	19.353 767	115.709	60.013	0	0	0	0	0
7	19.180 033	114.892	64.207	18.983	2.783	−7.833	1.952	23.103
8	19.171 222	114.736	63.602	27.047	3.466	−11.252	2.972	33.352
9	19.167 260	114.619	63.990	33.786	4.058	−14.364	4.077	42.140
10	19.165 782	114.658	63.679	37.870	4.298	−16.063	4.812	47.219
11	19.165 244	114.680	63.512	41.400	4.488	−17.523	5.434	51.621
12	19.165 079	114.681	63.381	44.276	4.633	−18.697	5.973	55.159
13	19.164 701	114.684	63.163	46.478	4.729	−19.539	6.417	57.776
14	19.164 677	114.685	63.238	48.459	4.813	−20.301	6.807	60.137
15	19.164 499	114.687	63.059	49.999	4.870	−20.854	7.137	61.905
16	19.164 467	114.687	63.063	51.368	4.919	−21.340	7.428	63.459
17	19.164 400	114.687	62.993	52.493	4.956	−21.717	7.679	64.704
18	19.164 370	114.687	62.957	53.476	4.987	−22.036	7.901	65.768
19	19.164 342	114.687	62.940	54.317	5.012	−22.297	8.097	66.658
20	19.164 323	114.687	62.917	55.049	5.032	−22.515	8.271	67.417
21	19.164 309	114.688	62.899	55.688	5.049	−22.698	8.427	68.066
22	19.164 299	114.688	62.897	56.250	5.063	−22.851	8.567	68.623
23	19.164 291	114.688	62.885	57.746	5.075	−22.981	8.692	69.105
24	19.164 287	114.688	62.889	57.187	5.085	−23.091	8.806	69.525
25	19.164 283	114.688	62.885	57.579	5.094	−23.185	8.909	69.891
26	19.164 281	114.688	62.888	57.931	5.101	−23.266	9.003	70.214
27	19.164 279	114.688	62.897	58.248	5.108	−23.335	9.088	70.500
28	19.164 278	114.688	62.898	58.534	5.113	−23.396	9.167	70.754
29	19.164 278	114.688	62.903	58.793	5.118	−23.448	9.239	70.982
30	19.164 277	114.688	62.903	59.029	5.123	−23.495	9.305	71.186

TABLE VII. E_{HF} and HOMO–LUMO gap (in E_h) and E_c (in mE_h) in n-boxium and n-hookium.

	n-boxium ($L = \pi$)				n-hookium ($k = 1$)			
	$n = 2$	$n = 3$	$n = 4$	$n = 5$	$n = 2$	$n = 3$	$n = 4$	$n = 5$
E_{HF}	3.48451	10.37969	22.42489	40.79205	2.74367	6.63671	12.12335	19.16428
H-L gap	4.01	5.28	6.47	7.61	1.75	1.72	1.69	1.67
$-E_c^{LDA1}$	46.1	72.5	99.4	126.5	42.2	65.9	90.1	114.7
$-E_c^{gLDA1}$	11.0	26.3	44.0	63.0	12.7	28.0	44.9	62.9
$-E_c^{MP2}$	8.3	23.1	41.8	62.8	10.8	26.0	43.7	63.0
$-E_c^{MP3}$	9.5	25.6	45.4	67.3	12.7	30.0	49.8	71.1
$-E_c^{FCI}$	9.8	26.2	46.1	68.0	13.5	31.8	52.4	74.3

We first discuss 2-boxium. Choosing $M = 8$ yields the HF orbitals

$$\psi_1(x) = 0.994844\,\phi_1(x) - 0.101256\,\phi_3(x) - 0.005729\,\phi_5(x)$$
$$- 0.000044\,\phi_7(x), \tag{43a}$$

$$\psi_2(x) = 0.999715\,\phi_2(x) - 0.023850\,\phi_4(x) + 0.000728\,\phi_6(x)$$
$$- 0.000176\,\phi_8(x), \tag{43b}$$

and Fig. 1 reveals that the density ρ has maxima at $x \approx \pm\pi/4$, indicating that an electron is likely to be found in these regions. LDA1 interprets these maxima as the most strongly correlated regions in the well and, through Eqs. (2) and (39), predicts the correlation energy

$$E_c^{LDA1} = \int_{-\pi/2}^{\pi/2} \rho(x)\varepsilon_c^{LDA1}(r_s)\,dx = -46.1 \text{ m}E_h. \tag{44}$$

In contrast, because the hole curvature η is strongly peaked at the center and edges of the box and is small near the density maxima, gLDA1 identifies the *center* of the box as the most correlated region and Eqs. (23) and (41) predict the much smaller correlation energy

$$E_c^{gLDA1} = \int_{-\pi/2}^{\pi/2} \rho(x)\varepsilon_c^{gLDA1}(r_s, \eta)\,dx = -11.0 \text{ m}E_h. \tag{45}$$

LDA1 and gLDA1 offer very different qualitative and quantitative descriptions of 2-boxium, but both perturbation theory ($E_c^{MP2} = -8.33$ mE_h and $E_c^{MP3} = -9.45$ mE_h) and near-exact calculations ($E_c^{FCI} = -9.82$ mE_h) support the gLDA1 picture.

We have also performed HF, LDA1, gLDA1, MP2, MP3, and FCI calculations on 3-, 4-, and 5-boxium and the density and curvature for 5-boxium are shown on the right of Fig. 1. Both functions oscillate much more rapidly but with much smaller amplitude than in 2-boxium, and it is easy to foresee that, as the number of electrons becomes large, both the density and the curvature will become increasingly uniform.

The convergence of the 5-boxium energies is shown in Table V and confirms the theoretical predictions of Table IV. The LDA1 energies, which depend only on the density $\rho(x)$, converge rapidly, changing by less than 1 μE_h beyond $M = 11$. The HF and gLDA energies, which depend on the orbitals (rather than the density) converge more slowly, achieving 1 μE_h convergence around $M = 20$. Because the occupied orbitals converge more rapidly than the virtual ones,[94] the O^4V^2 component of MP3 converges almost as fast as HF, the O^3V^3 component (which is negative) converges more slowly, and the O^2V^4 component (which is positive) even more slowly.[95] Because of the resulting differential cancellation,[96,97] the total 3rd-order contribution initially becomes more negative, reaches a minimum at $M = 13$, and rises thereafter. The MP2 energy is the most slowly converging, and changes by 60 μE_h between $M = 29$ and $M = 30$. It is interesting to note the almost perfectly linear growth of the third-order energies. Because the n-boxiums are large-gap systems, MP2 and MP3 work well, recovering more than 92% and 99% of the correlation energy in 5-boxium.

Our best estimates of the CBS limit HF and correlation energies are summarized in the left half of Table VII. Because LDA1 operates without the benefit of curvature information, it gravely overestimates the correlation energy, by between a
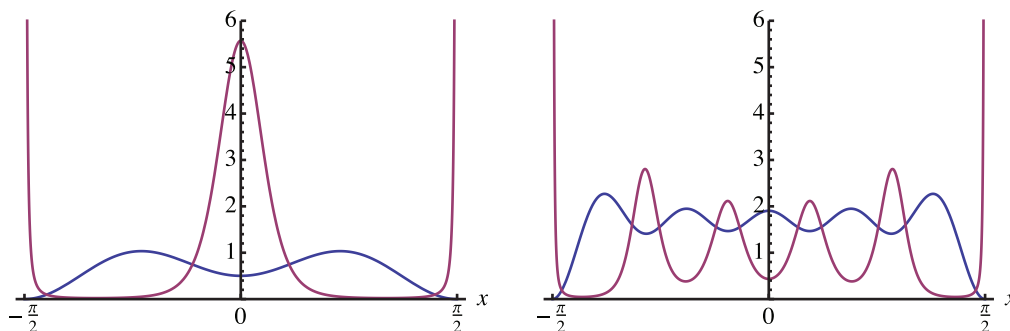
FIG. 1. HF density $\rho(x)$ (blue) and curvature $\eta(x)$ (red) in 2-boxium (left) and 5-boxium (right)
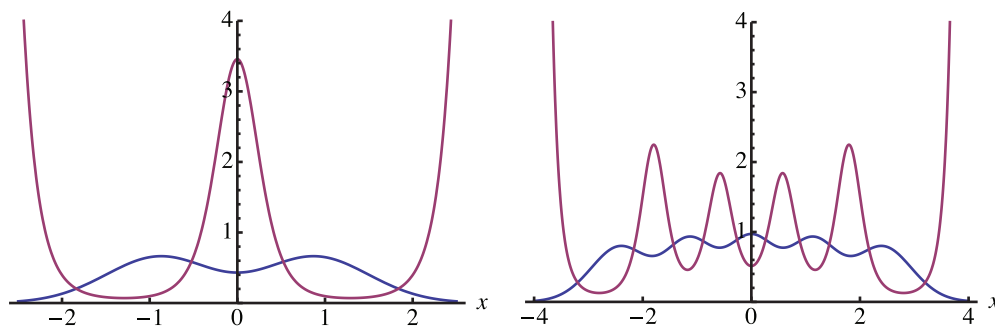
FIG. 2. HF density $\rho(x)$ (blue) and curvature $\eta(x)$ (red) in 2-hookium (left) and 5-hookium (right).

factor of five (for 2-boxium) and a factor of just under two (for 5-boxium). In contrast, gLDA1 is within 12% of the true correlation energy for all n-boxiums studied.

B. n-hookium

Electrons in 3D harmonic wells have been studied by numerous authors[98–112] but this is the first investigation of n electrons in a 1D harmonic well. The orbitals of 1-hookium are

$$\phi_m(x) = \frac{H_{m-1}(x)\exp(-x^2/2)}{\sqrt{\pi^{1/2}2^{m-1}(m-1)!}} \quad (m = 1, 2, 3, \ldots) \quad (46)$$

and the first M of these form a convenient orthonormal basis for expanding the HF orbitals in n-hookium. The antisymmetrized two-electron integrals $\langle \mu\sigma||\nu\lambda \rangle$ can be found in closed form (e.g., see Appendix B) and we have used these to perform SCF calculations with up to $M = 30$ basis functions. Our convergence criterion was max $|[\mathbf{P}, \mathbf{F}]| < 10^{-5}$.

We first discuss 2-hookium. Choosing $M = 8$ yields the HF orbitals

$$\psi_1(x) = 0.989962\,\phi_1(x) + 0.139577\,\phi_3(x) - 0.021464\,\phi_5(x)$$
$$+0.005740\,\phi_7(x), \quad (47a)$$

$$\psi_2(x) = 0.997679\,\phi_2(x) + 0.067586\,\phi_4(x) - 0.008026\,\phi_6(x)$$
$$+0.001894\,\phi_8(x), \quad (47b)$$

and Fig. 2 reveals that the density and curvature are softened versions of those in 2-boxium. As before, LDA1 interprets the density maxima as regions of strong correlation, predicting

$$E_c^{\text{LDA1}} = \int_{-\infty}^{\infty} \rho(x)\varepsilon_c^{\text{LDA1}}(r_s)\,dx = -42.2 \text{ m}E_{\text{h}}, \quad (48)$$

whereas gLDA1 finds that almost all of the correlation comes from a narrow region near the middle of the well and predicts

$$E_c^{\text{gLDA1}} = \int_{-\infty}^{\infty} \rho(x)\varepsilon_c^{\text{gLDA1}}(r_s, \eta)\,dx = -12.7 \text{ m}E_{\text{h}}. \quad (49)$$

As for 2-boxium, LDA1 and gLDA1 offer entirely different pictures of electron correlation but both perturbation theory ($E_c^{\text{MP2}} = -10.78$ mE_{h} and $E_c^{\text{MP3}} = -12.66$ mE_{h}) and near-exact calculations ($E_c^{\text{FCI}} = -13.55$ mE_{h}) agree that gLDA1 is closer to the truth.

We have also performed HF, LDA1, gLDA1, MP2, MP3, and FCI calculations on 3-, 4-, and 5-hookium and the density and curvature for 5-hookium are shown on the right of Fig. 2. As before, both functions oscillate more rapidly but with smaller amplitude than in 2-hookium and it is clear that, as the number of electrons becomes large, both functions will become increasingly uniform.[113]

The convergence of the 5-hookium energies is shown in Table VI. As in 5-boxium, the LDA1 energies converge most rapidly, followed by the HF and gLDA1 energies, then the O^4V^2, O^3V^3, and O^2V^4 components of the third-order energy, and finally the MP2 energy. However, each of these energies converges significantly more slowly than its 5-boxium analog. All of these observations are consistent with the theoretical predictions of Table IV. Because the n-hookiums are smaller gap systems, MP2 and MP3 are less successful than for n-boxium, recovering roughly 85% and 96% of the correlation energy in 5-hookium.

Our best estimates of the CBS limit HF and correlation energies are summarized in the right half of Table VII. As before, whereas LDA1 seriously overestimates the correlation energies, gLDA1 is within 15% of the true correlation energy in all cases. It is interesting to note that $|E_c(n\text{-hookium})| > |E_c(n\text{-boxium})|$ in all cases but that, whereas gLDA1 correctly predicts this trend, LDA1 reverses it.

VI. CONCLUDING REMARKS

The traditional LDA is exact by construction for an infinite uniform electron gas with Seitz radius r_s. However, it significantly overestimates the magnitudes of correlation energies in finite gases, such as those created when n electrons are placed on the surface of a $\mathcal{D}$-dimensional sphere. This overestimation, which becomes even more pronounced in non-uniform gases, led us to seek generalizations of the LDA which are exact for both infinite and finite gases and, in the present work, we have proposed that the local hole curvature η provides the necessary information to achieve this goal. For present purposes, we have extracted η from the HF wave function: this requires only the occupied HF orbitals.

By fitting accurately calculated correlation energies for systems of n electrons on a ring, we have constructed the generalized local density approximation for one-dimensional systems and this has yielded a correlation kernel $\varepsilon_c(r_s, \eta)$ and a corresponding functional which we call GLDA1. To this

point, we have considered only gases in which $\eta \leq 1$ and, consequently, the GLDA1 functional is not yet defined for gases with higher curvature. However, if we assume that the correlation kernel becomes flat, i.e., that $\varepsilon_c(r_s, \eta) = \varepsilon_c(r_s, 1)$ when $\eta > 1$, we obtain an approximation to GLDA1 which we call gLDA1.

We have applied the traditional LDA1 functional and the curvature-corrected gLDA1 functional to electrons trapped in 1D boxes or in 1D harmonic wells and, by comparing the predicted correlation energies with those obtained from MP2, MP3, and full CI calculations, we have discovered that gLDA1 is much more accurate than LDA1 in all cases.

We have also observed that gLDA1 tends to underestimate the magnitudes of correlation energies. This suggests that the true GLDA1 kernel continues to rise, i.e., that $|\varepsilon_c(r_s, \eta)| > |\varepsilon_c(r_s, 1)|$ but systematic examination of high-curvature ($\eta > 1$) gases is required to test this. Such exploration is an important topic for future research and will allow the GLDA1 functional to be completely defined and tested.

Although we have presented relatively few calculations here, and much more investigation is warranted, these preliminary results suggest that "curvature-corrected density functional theory (CC-DFT)" may offer an efficient pathway to improvements over existing functionals.

ACKNOWLEDGMENTS

APPENDIX A: CALCULATION OF MATRIX ELEMENTS

The matrix elements in Eq. (22) are expressed as expectation values of operators over the HF wave function. Therefore, because Φ^2 and its reduced density matrices, e.g.,

$$\rho_2(\theta_1, \theta_2) = \rho(\mathbf{r})^2 \left(1 - \left[\frac{\sin n(\theta_1 - \theta_2)/2}{n \sin(\theta_1 - \theta_2)/2} \right]^2 \right) \quad \text{(A1)}$$

have *finite* Fourier expansions, integrals of their products with Fourier expansions of operators reduce to *finite* sums.

The Fourier expansions of bounded operators on a unit ring are straightforward, e.g.,

$$r_{12}^2 = 2 - 2\cos(\theta_1 - \theta_2), \quad \text{(A2)}$$

$$\nabla r_{12} \cdot \nabla r_{12} = 1 + \cos(\theta_1 - \theta_2), \quad \text{(A3)}$$

$$r_{12} = -\frac{4}{\pi} \sum_{a=-\infty}^{\infty} \frac{e^{ia(\theta_1 - \theta_2)}}{4a^2 - 1}, \quad \text{(A4)}$$

$$\nabla r_{12} \cdot \nabla r_{13} = \left[\frac{4i}{\pi} \sum_{a=-\infty}^{\infty} \frac{ae^{ia(\theta_1 - \theta_2)}}{4a^2 - 1} \right] \left[\frac{4i}{\pi} \sum_{b=-\infty}^{\infty} \frac{be^{ib(\theta_1 - \theta_3)}}{4b^2 - 1} \right]. \quad \text{(A5)}$$

The expansions of unbounded operators, e.g.,

$$r_{12}^{-1} = -\frac{2}{\pi} \sum_{a=-\infty}^{\infty} \left(\sum_{p=1}^{|a|} \frac{1}{2p - 1} \right) e^{ia(\theta_1 - \theta_2)} \quad \text{(A6)}$$

are delicate (they converge only in the Cesàro mean[89]) but this is sufficient for our purposes because we require only a few of the low-order Fourier coefficients. The expansions of "cyclic" operators (e.g., $r_{12}r_{23}r_{31}$) are not simple products and must be derived separately.

Thus, for example, to find the $\langle \Phi | r_{12}r_{13} | \Phi \rangle$ integral in 3-ringium, the Fourier expansion

$$\Phi^2 = \frac{[2 - 2\cos(\theta_1 - \theta_2)][2 - 2\cos(\theta_1 - \theta_3)][2 - 2\cos(\theta_2 - \theta_3)]}{3!(2\pi)^3} \quad \text{(A7)}$$

is combined with Eq. (A4) to yield

$$\langle \Phi | r_{12}r_{13} | \Phi \rangle$$
$$= \frac{16}{\pi^2} \sum_{a=-2}^{2} \sum_{b=-2}^{2} \iiint \frac{e^{ia(\theta_1 - \theta_2)}}{4a^2 - 1} \frac{e^{ib(\theta_1 - \theta_3)}}{4b^2 - 1} \Phi^2 d\theta_1 d\theta_2 d\theta_3$$
$$= \frac{16384}{675\pi^2}. \quad \text{(A8)}$$

APPENDIX B: EXTRAPOLATION OF PERTURBATION ENERGIES

It is common these days to estimate the CBS limit of post-HF correlation energies by extrapolation.[114] Pioneering work by Schwartz,[115] Hill,[116] and Kutzelnigg and Morgan[117] showed that, for atoms in 3D, the second-order energy contributions from basis functions with angular momentum ℓ converge asymptotically as $(\ell + 1/2)^{-4}$.

While generating the data in Sec. V, we found that the MP2 and MP3 energies converge so slowly (Tables V and VI) that the CBS limit is not reached (within our 0.1 mE_h target accuracy), even with our largest ($M = 30$) basis set. This is particularly noticeable for n-hookium. We therefore needed to develop and apply appropriate extrapolation procedures.

To this end, we analyzed the convergence of the second-order energy

$$E^{(2)} = \sum_{r=3}^{\infty} \sum_{s=r+1}^{\infty} \frac{\langle 12||rs \rangle^2}{\epsilon_1 + \epsilon_2 - \epsilon_r - \epsilon_s} \quad \text{(B1)}$$

obtained from the non-interacting orbitals and orbital energies in 2-boxium and 2-hookium. In n-hookium, the double-bar integral is

$$\langle 12||rs \rangle = \frac{(-1)^{(r-s+1)/2}\sqrt{2}}{\pi} \frac{\Gamma((r + s - 2)/2)}{\sqrt{\Gamma(r)\Gamma(s)}}, \quad \text{(B2)}$$

if $r + s$ is odd but it vanishes if $r + s$ is even. The orbital energies are given by $\varepsilon_k = k - 1/2$. By substituting these expressions into (B1) and making use of Stirling's approximation,[89]

one can show that the error introduced by truncating the basis after M functions is

$$\Delta E_M^{(2)} = \sum_{r=3}^{M} \sum_{s=r+1}^{M} \frac{\langle 12||rs \rangle^2}{\epsilon_1 + \epsilon_2 - \epsilon_r - \epsilon_s} - E^{(2)}$$

$$\sim \frac{1}{3(\pi M)^{3/2}} + O(M^{-2}). \tag{B3}$$

The closed-form expression for the $\langle 12||rs \rangle$ integral in n-boxium is cumbersome but a similar analysis reveals that the analogous truncation error is $O(M^{-3})$. The truncation errors in the third-order energy can be found in the same way and all of our results are summarized in Table IV.

The MP2, MP3, and FCI energies obtained with our largest basis sets conform to these analytical predictions and allowed us to extrapolate reliably to the CBS energies given in Table VII. The good agreement between our extrapolated FCI energies and QMC energies further increases our confidence in these results.

[1] R. G. Parr and W. Yang, *Density-Functional Theory of Atoms and Molecules* (Oxford, Clarendon Press, 1989).
[2] E. Fermi, Z. Phys. **36**, 902 (1926).
[3] L. H. Thomas, Proc. Cambridge Philos. Soc. **23**, 542 (1927).
[4] E. Wigner, Phys. Rev. **46**, 1002 (1934).
[5] W. Macke, Z. Naturforsch. A **5a**, 192 (1950).
[6] D. Bohm and D. Pines, Phys. Rev. **92**, 609 (1953).
[7] D. Pines, Phys. Rev. **92**, 626 (1953).
[8] M. Gell-Mann and K. A. Brueckner, Phys. Rev. **106**, 364 (1957).
[9] D. F. DuBois, Ann. Phys. **7**, 174 (1959).
[10] W. J. Carr, Jr. and A. A. Maradudin, Phys. Rev. **133**, A371 (1964).
[11] S. Misawa, Phys. Rev. **140**, A1645 (1965).
[12] L. Onsager, L. Mittag, and M. J. Stephen, Ann. Phys. **18**, 71 (1966).
[13] A. Isihara and D. Y. Kojima, Z. Phys. B **21**, 33 (1975).
[14] D. Y. Kojima and A. Isihara, Z. Phys. B **25**, 167 (1976).
[15] Y. Wang and J. P. Perdew, Phys. Rev. B **43**, 8911 (1991).
[16] G. G. Hoffman, Phys. Rev. B **45**, 8730 (1992).
[17] T. Endo, M. Horiuchi, Y. Takada, and H. Yasuhara, Phys. Rev. B **59**, 7367 (1999).
[18] P. Ziesche and J. Cioslowski, Physica A **356**, 598 (2005).
[19] P. F. Loos and P. M. W. Gill, Phys. Rev. B **84**, 033103 (2011).
[20] R. K. P. Zia, J. Phys. C **6**, 3121 (1973).
[21] M. L. Glasser, J. Phys. C: Solid State Phys. **10**, L121 (1977).
[22] A. K. Rajagopal and J. C. Kimball, Phys. Rev. B **15**, 2819 (1977).
[23] A. Isihara and T. Toyoda, Ann. Phys. **106**, 394 (1977).
[24] A. Isihara and T. Toyoda, Ann. Phys. **114**, 497 (1978).
[25] A. Isihara and L. Ioriatti, Phys. Rev. B **22**, 214 (1980).
[26] M. L. Glasser, J. Comput. Appl. Math. **10**, 293 (1984).
[27] M. Seidl, Phys. Rev. B **70**, 073101 (2004).
[28] S. Chesi and G. F. Giuliani, Phys. Rev. B **75**, 153306 (2007).
[29] P. F. Loos and P. M. W. Gill, Phys. Rev. B **83**, 233102 (2011).
[30] M. M. Fogler, Phys. Rev. Lett. **94**, 056405 (2005).
[31] G. E. Astrakharchik and M. D. Girardeau, Phys. Rev. B **83**, 153303 (2011).
[32] P. F. Loos, J. Chem. Phys. **138**, 064108 (2013).
[33] R. A. Coldwell-Horsfall and A. A. Maradudin, J. Math. Phys. **1**, 395 (1960).
[34] W. J. Carr, Jr., Phys. Rev. **122**, 1437 (1961).
[35] W. J. Carr, Jr., R. A. Coldwell-Horsfall, and A. E. Fein, Phys. Rev. **124**, 747 (1961).
[36] G. Meissner, H. Namaizawa, and M. Voss, Phys. Rev. B **13**, 1370 (1976).
[37] L. Bonsall and A. A. Maradudin, Phys. Rev. B **15**, 1959 (1977).
[38] D. Ceperley, Phys. Rev. B **18**, 3126 (1978).
[39] D. M. Ceperley and B. J. Alder, Phys. Rev. Lett. **45**, 566 (1980).
[40] B. Tanatar and D. M. Ceperley, Phys. Rev. B **39**, 5005 (1989).
[41] Y. Kwon, D. M. Ceperley, and R. M. Martin, Phys. Rev. B **48**, 12037 (1993).
[42] G. Ortiz and P. Ballone, Phys. Rev. B **50**, 1391 (1994).
[43] F. Rapisarda and G. Senatore, Aust. J. Phys. **49**, 161 (1996).
[44] Y. Kwon, D. M. Ceperley, and R. M. Martin, Phys. Rev. B **58**, 6800 (1998).
[45] G. Ortiz, M. Harris, and P. Ballone, Phys. Rev. Lett. **82**, 5317 (1999).
[46] D. Varsano, S. Moroni, and G. Senatore, Europhys. Lett. **53**, 348 (2001).
[47] M. W. C. Foulkes, L. Mitas, R. J. Needs, and G. Rajagopal, Rev. Mod. Phys. **73**, 33 (2001).
[48] C. Attaccalite, S. Moroni, P. Gori-Giorgi, and G. B. Bachelet, Phys. Rev. Lett. **88**, 256601 (2002).
[49] F. H. Zong, C. Lin, and D. M. Ceperley, Phys. Rev. E **66**, 036703 (2002).
[50] L. Mitas, Phys. Rev. Lett. **96**, 240402 (2006).
[51] N. D. Drummond and R. J. Needs, Phys. Rev. Lett. **102**, 126402 (2009).
[52] A. Lüchow, R. Petz, and A. Schwarz, Z. Phys. Chem. **224**, 343 (2010).
[53] J. J. Shepherd, G. Booth, A. Grüneis, and A. Alavi, Phys. Rev. B **85**, 081103 (2012).
[54] S. H. Vosko, L. Wilk, and M. Nusair, Can. J. Phys. **58**, 1200 (1980).
[55] J. P. Perdew and A. Zunger, Phys. Rev. B **23**, 5048 (1981).
[56] J. P. Perdew and Y. Wang, Phys. Rev. B **45**, 13244 (1992).
[57] J. Sun, J. P. Perdew, and M. Seidl, Phys. Rev. B **81**, 085123 (2010).
[58] P. M. W. Gill and P. F. Loos, Theor. Chem. Acc. **131**, 1069 (2012).
[59] A. J. Pérez-Jiménez, F. Moscardó, J. C. Sancho-García, L. P. Abia, E. San-Fabián, and J. M. Pérez-Jordá, J. Chem. Phys. **114**, 2022 (2001).
[60] R. Colle and O. Salvetti, Theor. Chim. Acta **37**, 329 (1975).
[61] H. Stoll, E. Golka, and H. Preuss, Theor. Chim. Acta **55**, 29 (1980).
[62] A. D. Becke, Int. J. Quantum Chem. **23**, 1915 (1983).
[63] W. L. Luken and J. C. Culberson, Theor. Chim. Acta **66**, 279 (1984).
[64] J. F. Dobson, J. Chem. Phys. **94**, 4328 (1991).
[65] P. F. Loos and P. M. W. Gill, Phys. Rev. A **79**, 062517 (2009).
[66] P. F. Loos and P. M. W. Gill, Phys. Rev. Lett. **103**, 123008 (2009).
[67] P. F. Loos and P. M. W. Gill, Chem. Phys. Lett. **500**, 1 (2010).
[68] P. F. Loos and P. M. W. Gill, Mol. Phys. **108**, 2527 (2010).
[69] P. F. Loos and P. M. W. Gill, Phys. Rev. Lett. **105**, 113001 (2010).
[70] P. F. Loos and P. M. W. Gill, J. Chem. Phys. **135**, 214111 (2011).
[71] P. F. Loos and P. M. W. Gill, Phys. Rev. Lett. **108**, 083002 (2012).
[72] P. F. Loos and P. M. W. Gill, J. Chem. Phys. **138**, 164124 (2013).
[73] C. A. Coulson and A. H. Neilson, Proc. Phys. Soc. (London) **78**, 831 (1961).
[74] A. J. Coleman, Int. J. Quantum Chem., Symp. **1**, 457 (1967).
[75] J. P. Perdew and Y. Wang, Phys. Rev. B **46**, 12947 (1992).
[76] J. Cioslowski and G. Liu, J. Chem. Phys. **109**, 8225 (1998).
[77] A. M. Lee and P. M. W. Gill, Chem. Phys. Lett. **313**, 271 (1999).
[78] P. M. W. Gill, A. M. Lee, N. Nair, and R. D. Adamson, J. Mol. Struct. Theochem **506**, 303 (2000).
[79] P. M. W. Gill, D. P. O'Neill, and N. A. Besley, Theor. Chem. Acc. **109**, 241 (2003).
[80] P. M. W. Gill, D. L. Crittenden, D. P. O'Neill, and N. A. Besley, Phys. Chem. Chem. Phys. **8**, 15 (2006).
[81] P. M. W. Gill, Annu. Rep. Prog. Chem., Sect. C **107**, 229 (2011).
[82] A. J. Proud, M. P. Walker, and J. K. Pearson, Int. J. Quantum Chem. **113**, 76 (2013).
[83] E. R. Davidson, *Reduced Density Matrices in Quantum Chemistry* (Academic, New York, 1976).
[84] In response to a referee, we have calculated the exact and HF curvatures in 2-ringium for several values of the ring radius R. The HF curvature is $\eta_{HF} = 3/4$ for all R. In contrast, the exact curvature diminishes from $\eta = 3/4$ at $R = 0$, to $\eta = 9\pi/(32 + 12\pi) \approx 0.406$ at $R = 1/2$, to $\eta = 18\pi/(64\sqrt{6} + 51\pi) \approx 0.178$ at $R = \sqrt{3/2}$, and finally to $\eta = 0$ at $R = \infty$.
[85] R. J. Needs, M. D. Towler, N. D. Drummond, and P. L. Rios, J. Phys. Condens. Matter **22**, 023201 (2010).
[86] P. J. Knowles and N. C. Handy, Chem. Phys. Lett. **111**, 315 (1984).
[87] P. J. Knowles and N. C. Handy, Comput. Phys. Commun. **54**, 75 (1989).
[88] J. Cioslowski, J. Chem. Phys. **136**, 044109 (2012).
[89] *NIST Handbook of Mathematical Functions*, edited by F. W. J. Olver, D. W. Lozier, R. F. Boisvert, and C. W. Clark (Cambridge University Press, New York, 2010).
[90] W. Kutzelnigg, Int. J. Quantum Chem. **51**, 447 (1994).
[91] L. K. McKemmish and P. M. W. Gill, J. Chem. Theory Comput. **8**, 4891 (2012).
[92] W. Kutzelnigg, Int. J. Quantum Chem. **113**, 203 (2013).
[93] E. A. Salter, G. W. Trucks, and D. S. Cyphert, Am. J. Phys. **69**, 120 (2001).
[94] J. Deng and P. M. W. Gill, J. Chem. Phys. **134**, 081103 (2011).
[95] The symbols "O" and "V" refer to the number of occupied and virtual orbitals, respectively. The $O^4 V^2$ component, for example, involves four sums over occupied orbitals and two over virtual orbitals.
[96] J. Noga and W. Kutzelnigg, J. Chem. Phys. **101**, 7738 (1994).

[97]A. Köhn and D. P. Tew, J. Chem. Phys. **133**, 174117 (2010).
[98]N. R. Kestner and O. Sinanoğlu, Phys. Rev. **128**, 2687 (1962).
[99]E. Santos, Anal. R. Soc. Esp. Fis. Quim. **64**, 177 (1968).
[100]R. J. White and W. Byers Brown, J. Chem. Phys. **53**, 3869 (1970).
[101]J. M. Benson and W. Byers Brown, J. Chem. Phys. **53**, 3880 (1970).
[102]S. Kais, D. R. Herschbach, and R. D. Levine, J. Chem. Phys. **91**, 7791 (1989).
[103]M. Taut, Phys. Rev. A **48**, 3561 (1993).
[104]S. Ivanov, K. Burke, and M. Levy, J. Chem. Phys. **110**, 10262 (1999).
[105]J. Cioslowski and K. Pernal, J. Chem. Phys. **113**, 8434 (2000).
[106]T. M. Henderson, K. Runge, and R. J. Bartlett, Chem. Phys. Lett. **337**, 138 (2001).

[107]D. P. O'Neill and P. M. W. Gill, Phys. Rev. A **68**, 022505 (2003).
[108]J. Katriel, S. Roy, and M. Springborg, J. Chem. Phys. **123**, 104104 (2005).
[109]P. M. W. Gill and D. P. O'Neill, J. Chem. Phys. **122**, 094110 (2005).
[110]S. Ragot, J. Chem. Phys. **128**, 164104 (2008).
[111]P. F. Loos and P. M. W. Gill, J. Chem. Phys. **131**, 241101 (2009).
[112]J. Cioslowski, J. Chem. Phys. **139**, 224108 (2013).
[113]P. F. Loos and P. M. W. Gill, Mol. Phys. **110**, 2337 (2012).
[114]T. Helgaker, W. Klopper, H. Koch, and J. Noga, J. Chem. Phys. **106**, 9639 (1997).
[115]C. Schwartz, Phys. Rev. **126**, 1015 (1962).
[116]R. N. Hill, J. Chem. Phys. **83**, 1173 (1985).
[117]W. Kutzelnigg and J. D. Morgan III, J. Chem. Phys. **96**, 4484 (1992).